

Tides on Filchner-Ronne Ice Shelf from ERS radar altimetry

Helen Amanda Fricker¹ and Laurie Padman²

Received 2 October 2001; accepted 2 January 2002; published 29 June 2002.

[1] We use harmonic analysis of 8 years of ERS satellite radar altimeter (RA) data at orbital crossovers to retrieve complex amplitude (amplitude and phase) coefficients for several major tidal harmonics over the Filchner-Ronne Ice Shelf (FRIS), Antarctica. We describe a method for estimating the accuracy of this method, which ranges from ~ 2 to 8 cm per harmonic. A comparison between M_2 complex amplitude from a recent ocean model and from our ERS RA analyses identifies two regions of the FRIS where the RA data are inconsistent with the model. In both regions the differences can be attributed to incorrect specification of the grounding line location in the model. Our study demonstrates the value of ERS RA data in Antarctic ice shelf tide modeling, and the potential for future altimeter satellites with high polar orbits to contribute to the definition of global tide height variations. *INDEX TERMS:* 4207 Oceanography: General: Arctic and Antarctic oceanography; 4294 Oceanography: General: Instruments and techniques; 9310 Information Related to Geographic Region: Antarctica

1. Introduction

[2] Ocean tides are the primary cause of high-frequency height variability of the floating ice shelves surrounding Antarctica, and tidal height variability often exceeds the seasonal to multi-year changes that we attempt to observe using satellite-based sensors. Data from radar altimeter (RA) and synthetic aperture radar (SAR) instruments, such as those on the European Space Agency's ERS satellites, are routinely used to monitor ice shelf surface elevation change and flow rates, respectively [e.g., Fricker *et al.*, 2000, Rignot and MacAyeal, 1998]. However, typical satellite repeat periods (3, 35 and 168 days for ERS) are much longer than the time-scale of ocean tides (~ 1 day), and so the tidal height variability is aliased into the satellite-derived time series. Removal of the tidal signal from RA and interferometric SAR data collected over ice shelves is therefore an essential step in detecting true changes on seasonal and longer time scales.

[3] Removal of tides from satellite data requires an accurate tidal prediction model. Most recent global models are constrained to fit TOPEX/Poseidon (T/P) RA data and consequently provide accurate estimates of ocean tide over the deep ocean [Shum *et al.*, 1997]. However, the turning latitude for the T/P satellite is $\sim 66^\circ\text{S}$, which excludes all of the major Antarctic ice shelves. Ice shelf tides are difficult to model because of the paucity of good bathymetry data (including water column thickness in the sub ice shelf cavity), and a lack of in situ measurements that could be used in assimilation studies. Comparisons between one assimilation tidal model [Padman *et al.*, 2002] and GPS measurements on ice shelves in various regions suggest that further improvement in predictive skill is needed [King, 2001].

[4] In this paper we report on a preliminary study to assess whether RA data from the ERS satellites can provide useful tidal information for the Antarctic ice shelves. Andersen [1994] and Smith [1999] have previously used ERS 35-day repeat RA data to retrieve tides over the open ocean, but the process has never been applied to the ice shelves. We focus on the large Filchner-Ronne Ice Shelf (FRIS), which floats on the southern Weddell Sea.

2. Data

[5] Radar altimeters estimate the range from the spacecraft to the Earth's surface by measuring the two-way time delay between a transmitted and received microwave pulse. The measured range is to the average surface elevation in the "pulse-limited" RA footprint, whose diameter is about 5–10 km for ERS over an ice shelf, depending on the surface roughness. We used RA data processed by the Ice Altimetry group at the Goddard Space Flight Center (GSFC). The range had been converted into height above the WGS-84 ellipsoid with knowledge of the satellite altitude, corrections for instrument and atmospheric delays, and the body tide (see Fricker *et al.* [2000] for details of corrections). No correction had been applied for the ocean-load tide. The data had been 'retracked' using the GSFC β -parameter retracking algorithm [Martin *et al.*, 1983] to find the location on the return waveform best corresponding to the true surface. We rejected waveforms that had not been successfully retracked or were classed as specular. This eliminated returns from regions close to the ice margins where the surface is rougher, and regions which may contain meltstreams.

[6] We restricted our analysis to RA height data interpolated to the intersection points of ascending and descending ERS tracks ("crossovers"). The reasons for this were that over the FRIS the crossover distribution is dense and the temporal sampling at the crossovers is better than elsewhere, and data volume is significantly reduced. At lower latitudes where crossover spacing is greater, the additional information available in the along-track signal would be a valuable addition to the tidal analysis. We used crossovers between orbits within the same repeat cycle, thus reducing redundancy in the use of each data point, and limiting the time delay between the two tracks at each crossover to less than the repeat period. We used RA data for the period 28 December 1991 to 31 March 2000 (Table 1) for the present study. The 3-day repeat period does not have good spatial coverage but provides high temporal resolution at a few locations. The 35-day repeat period is the most useful for tidal analyses. Although the 168-day repeat period is long, the orbit contains a sub-cycle of ~ 35 days and produces a large number of crossovers.

3. Method

[7] We assume that the ice shelf responds hydrostatically to changes in the ocean surface height. This is valid over most of the ice shelf with the exception of the flexural boundary region, within a few kilometers of the fully grounded ice. At each crossover we obtained the time (t_1, t_2) and the heights (h_1, h_2) of the two intersecting tracks by locating the two nearest RA records on either side of the crossover location, for each track, and interpolating between them. The height difference, $\delta h(t_1, t_2) = h_2(t_2) - h_1(t_1)$,

¹Institute of Geophysics and Planetary Physics, Scripps Institution of Oceanography, University of California, San Diego, La Jolla, CA, USA.

²Earth and Space Research, Seattle, WA, USA.

Table 1. Dates and Repeat Periods for ERS Data Used for Tidal Analysis

Satellite	RP	Dates
ERS-1	3	28 Dec 1991–30 Mar 1992 and 23 Dec 1993–10 April 1994
ERS-1	35	14 Apr 1992–21 Dec 1993 and 21 Mar 1995–02 Jun 1996
ERS-1	168	10 April 1994–21 Mar 1995
ERS-2	35	21 April 1995–31 Mar 2000

Repeat periods (RP) are exact multiples of one day.

can be expressed as a sum of n sinusoidal tidal harmonics plus an error term, i.e.,

$$\delta h(t_1, t_2) = \sum_{i=1}^n a_i(\cos(\omega_i t_2) - \cos(\omega_i t_1)) + \sum_{i=1}^n b_i(\sin(\omega_i t_2) - \sin(\omega_i t_1)) + \varepsilon,$$

where a_i and b_i are the amplitudes of the cosine and sine terms for the i 'th tidal frequency, ω_i , and t is referenced to the start of 1992 (denoted ' t_0 '). The residual term, ε , includes non-tidal sources of height variability, RA noise, and tidal harmonics that contribute to the signal but are excluded from the analysis. For the dominant 35-day repeat orbit, each crossover typically had between 30 and 60 values in its time series.

[8] The fitting algorithm seeks values of $\{a_i; i = 1, 2, \dots, n\}$ and $\{b_i; i = 1, 2, \dots, n\}$ that minimize the sum of the squared residuals, $\sum \varepsilon^2$, for a given set of δh . The analysis can be applied to δh data from a single crossover location, or to all values within a given search radius (r_s) of the point for which a tidal analysis is sought. The algorithm searches for the M_2 , K_2 , N_2 , O_1 , K_1 , and Q_1 tides. The S_2 tide (period = 12.000 h) cannot be evaluated because it is aliased to zero frequency by the ERS orbit. The P_1 tide is not included because its energy, and that of the annual cycle (S_a), are correlated with K_1 [Smith, 1999; his Table 4.1]. We include K_1 in the analysis to capture the combined contributions from K_1 , P_1 , and S_a . The semiannual cycle, S_{sa} , is inseparable from K_2 , but is insignificant for present purposes (<1 cm amplitude) based on analysis of long records from in situ tide gauges in the northern Weddell Sea.

[9] The harmonics chosen for the fitting procedure exclude those that modulate some constituents through the period of the nodal tide (~ 18.6 y), however some of this energy will be incorporated into the complex amplitude of the fitted tidal harmonic because the record length (~ 8 y) is shorter than the period of the nodal tide. We make no nodal corrections to ERS-derived complex amplitudes. Once $\{a_i\}$ and $\{b_i\}$ are found, these coefficients are converted to amplitude and phase (relative to t_0), then phase is converted to Greenwich phase lag based on known astronomical phases at $t = t_0$.

[10] To find the optimum value for r_s and to determine the accuracy of our method, we tested our algorithm on a synthetic height dataset derived from the Circum-Antarctic Tidal Simulation Version 01.01 (CATS01.01), an updated version of the CATS model described by Rignot *et al.* [2000]. For each crossover, $h_1(t_1)$ and $h_2(t_2)$ were predicted, using t_1 and t_2 from the RA dataset. Gaussian noise was added to h_1 and h_2 to simulate instrument measurement error and non-tidal variability. The standard deviation of the noise distribution was 0.7 m, based on a precision of 0.49 m for a single ERS RA measurement over ice shelves [Scott *et al.*, 1994], and taking into account the non-tidal sources of noise such as the inverse barometer effect [Rignot *et al.*, 2000]. The best results were obtained using values of $r_s \approx 25$ –50 km for most of the FRIS, with the smaller value being acceptable close to the turning latitude due to the convergence of the satellite ground tracks.

4. Results

[11] We know of no long-duration (>1 month) direct measurements of tide height for the FRIS, although some estimates have

been made from tiltmeter records and combined tiltmeter/gravimeter studies [Doake, 1992]. Instead of comparing with in situ data, therefore, we compared ERS-derived tides and CATS01.01 as a means of assessing the performance of ERS RA analysis over the larger area of the FRIS. The most energetic tide in the FRIS tidal fields is the semidiurnal M_2 [Robertson *et al.*, 1998], whose amplitude ranges from >160 cm in the southwest corner, to 0 cm (an amphidromic point) near the Ronne ice front near 57°W . The M_2 tide evaluated from ERS RA crossover data (using $r_s = 50$ km over the entire FRIS), is generally consistent with CATS01.01 (Figure 2). The CATS model provides ocean tides only (surface height relative to the deformable seabed), whereas the ERS analysis retrieves the difference of the ocean tide and the ocean-load tide. While the ratio of ocean-load tide to ocean tide is spatially variable, a sufficient approximation for the present study is ~ 0.05 [Ray and Sanchez, 1989]. Thus, the CATS01.01 ocean tide predictions have been scaled by 0.95 for direct comparison with ERS-derived tide. The CATS model is known to predict tide heights quite well in the Weddell Sea near and north of the FRIS ice front [Padman and Kottmeier, 2000], so we took the general agreement between the ERS-derived fields and the model as confirmation that our analysis of ERS RA data was working in this region.

[12] We illustrate the accuracy of our coefficient retrieval for all analyzed tidal harmonics by examining the results in detail at two sites: a region of large-amplitude tides in the southwest corner of the Ronne Ice Shelf (T1 in Figure 1; Table 2) and a region of more typical tides in the central Ronne Ice Shelf (T2 in Figure 1; Table 3). In these tables the ‘‘RMS difference’’ for each harmonic is the RMS amplitude of the sinusoidal difference signal between the ERS analysis and CATS01.01. We used this quantity because it combines the errors in both amplitude and phase for the two signals being compared. Our tests on the synthetic dataset gave us accuracy values for the coefficient retrieval for each harmonic, and that quantity is given in the last column in parentheses. We interpret an RMS difference greater than the accuracy value as a significant difference between ERS and modeled tides. For the two sites described in Tables 2 and 3, only the ERS-derived M_2 in the energetic tidal region (T1) is significantly different from CATS01.01.

5. Discussion

[13] The ERS time series is now long enough (>8 years) to extract useful tidal information over the FRIS by harmonic analysis of RA-derived height difference variability. Tests indicate that 6 tidal harmonics (M_2 , O_1 , K_1 , K_2 , N_2 , Q_1) can be retrieved with RMS accuracies of ~ 2 –8 cm per harmonic. The ERS orbit imposes some significant limitations on tidal retrieval

Table 2. Tidal Amplitude (cm) and Greenwich Phase Lag ($^\circ$) of the 8 Major Tidal Harmonics from CATS01.01 and ERS RA for a Region of Energetic Tides (73.0°W , 80.1°S : T1 in Figure 1)

	CATS01.01 (amp./phase)	ERS (amp./phase)	RMS difference
M_2	145/63	152/59	9 (5)
S_2	93/89	Not analyzed	–
K_2	26/91	19/73	7 (8)
N_2	24/45	25/44	1 (5)
O_1	40/50	37/53	3 (6)
K_1	45/65	41/80	9 (8)
P_1	15/66	Not analyzed	–
Q_1	10/46	10/59	2 (4)

The search radius is $r_s = 25$ km. The measured RMS difference (cm) is compared with the RMS error (shown in parentheses) that arises from tests based on sampling the CATS01.01 field at the same times as the ERS RA (see text).

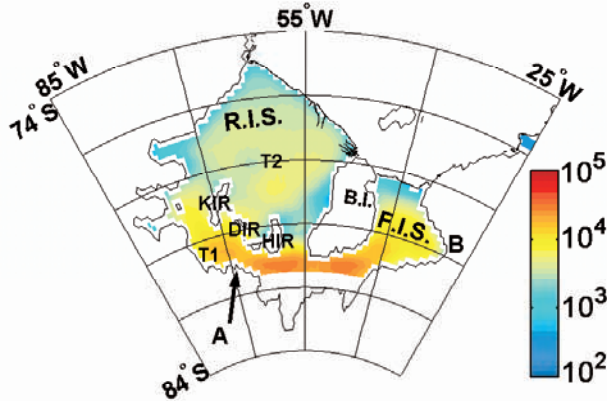


Figure 1. (opposite) Location of principal geographic features discussed in the text: RIS, Ronne Ice Shelf; FIS, Filchner Ice Shelf; BI, Berkner Island; KIR, Korff Ice Rise; DIR, Doake Ice Rumples; and HIR, Henry Ice Rise. The “island” north of Berkner Island is a set of grounded icebergs that were present during most of the 1990s. Two points chosen for detailed study in Tables 2 and 3 are shown: T1 and T2. The outlet of Institute Ice Stream (A) and the area around the outlets of Slessor Glacier and the Bailey Ice Stream (B) are indicated. Background coloring indicates the number of crossover pairs used in tidal analysis at each point, with a search radius of $r_s \approx 50$ km. Density increases significantly towards the ERS turning latitude of $\sim 81.5^\circ\text{S}$, and so the crossover technique is more powerful in this region. Note that the ERS orbit does not capture all of the FRIS grounding zone.

using the harmonic method [Smith, 1999]: the S_2 tide cannot be retrieved at all because it is aliased to zero frequency, and we cannot separate K_1 from the P_1 tide and the annual cycle. These limitations in tidal harmonic retrieval imply that we cannot use harmonic analysis of ERS data to create a predictive model of tide heights.

[14] Although we cannot create full tide models from these data, the ERS-derived fields for individual harmonics, notably M_2 , suggest ways in which tide models can be improved. Significant differences between ERS-derived and modeled M_2 complex amplitude were found in two regions of the FRIS: in the southwest corner of the Ronne Ice Shelf, south of the Korff Ice Rise

(near A in Figure 1); and in the embayment forming the eastern portion of the Filchner Ice Shelf (near B in Figure 1). In the former case the error in CATS01.01 appears to be due to the absence of a grounded region near the outlet of the Institute Ice Stream, near 80.7°S , 71°W . This grounded region is apparent in both seismic survey data [Johnson and Smith, 1997] and in our analyses of ERS crossover data for single crossover locations, and so should be incorporated into the ice shelf cavity geometry for future runs of CATS. In the latter case, adjusting the Filchner Ice Shelf grounding line in CATS to match recent suggested modifications [Gray *et al.*, 2002] may improve the fit between modeled and measured values in this region. Note that any model

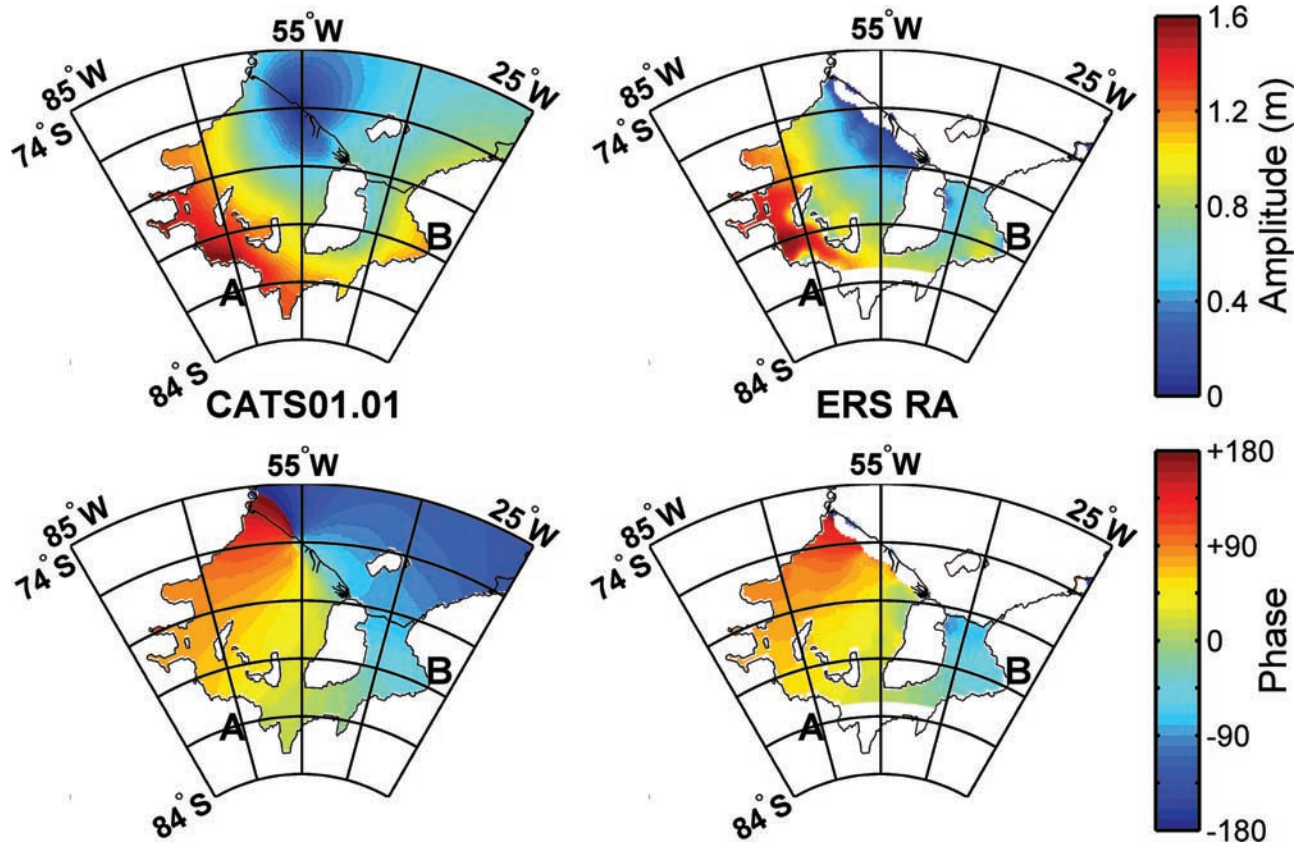


Figure 2. Comparison of M_2 tidal amplitude and “modified” Greenwich phase from CATS01.01 (left panels) and ERS crossover analysis (right panels). Phase is shifted by 180° to simplify visual comparison of modeled and measured phase under the FRIS. Areas for which the mean absolute value (m.a.v.) of the predicted tide height is less than $1/3$ of the m.a.v. of the total RA height signal are not contoured. This excludes a band about 80 km wide along the Ronne ice front. Points marked A and B are as indicated in Figure 1.

Table 3. Same as Table 2, but for a Region of More Typical Tides (60°W, 78°S: T2 in Figure 1) and $r_s = 50$ km.

	CATS01.01 (amp./phase)	ERS (amp./phase)	RMS difference
M ₂	63/60	59/61	3 (5)
S ₂	37/89	Not analyzed	–
K ₂	11/88	9/71	2 (3)
N ₂	11/42	12/56	2 (2)
O ₁	31/48	24/54	5 (6)
K ₁	33/63	33/46	7 (7)
P ₁	11/64	Not analyzed	–
Q ₁	8/43	4/59	3 (3)

geometry amendments suggested by our interpretation of the M₂ ERS-derived coefficients should improve the model prediction for all tidal harmonics.

6. Conclusions and Remarks

[15] This study demonstrates that harmonic analysis of ERS RA data provides reasonably accurate values of the coefficients for several major tidal harmonics over the Filchner-Ronne Ice Shelf. The RA data can also be useful for identifying weaknesses in existing tide models in the Antarctic. Improved solutions may be possible by using the response method of tidal analysis [e.g., Andersen, 1994], and by including all RA data in the analysis. Existing tide models may also be improved through formal assimilation of ice shelf RA measurements. Data from the Geoscience Laser Altimeter System (GLAS), to be launched on ICESat in late 2002, will extend the altimetric time series over the ice shelves for at least another 3 years. The higher accuracy of GLAS relative to the ERS RA, combined with its coverage to a higher latitude that encompasses all Antarctic ice shelves, is expected to significantly improve tide models for the ice shelves.

[16] **Acknowledgments.** ERS radar altimeter data is copyright to the European Space Agency and was provided by Jay Zwally and the Ice Altimetry group of Code 971 at the Goddard Space Flight Center. Glenn Hyland (Australian Antarctic Division) provided the RA crossover algorithm. Work at Earth and Space Research was supported by NASA (NAG5-7790) and the NSF Office of Polar Programs (OPP-9896006), and work at SIO by NASA grant NAS5-99006 to GLAS Team Member J.-B. Minster. We are grateful to Arthur Smith, Laurence Gray, and Gary Egbert for their helpful comments on this manuscript.

References

- Andersen, O. B., Ocean tides in the northern North Atlantic and adjacent seas from ERS 1 altimetry, *J. Geophys. Res.*, *99*, 22,557–22,573, 1994.
- Doake, C. S. M., Gravimetric tidal measurements on Filchner Ronne Ice Shelf, Filchner-Ronne Ice Shelf Program, Rep. 6, pp. 34–39, Alfred-Wegener-Inst., Bremerhaven, Germany, 1992.
- Fricke, H. A., G. Hyland, R. Coleman, and N. W. Young, Digital elevation models for the Lambert Glacier-Amery Ice Shelf system, East Antarctica, from ERS-1 satellite radar altimetry, *J. Glaciol.*, *46*(155), 553–560, 2000.
- Gray, A. L., N. Short, R. A. Bindschadler, I. Joughin, L. Padman, P. Vornberger, and A. Khananian, RADARSAT interferometry for Antarctic grounding zone mapping, *Ann. Glaciol.*, *34*, in press, 2002.
- Johnson, M. R., and A. M. Smith, Seabed topography under the southern and western Ronne Ice Shelf, derived from seismic surveys, *Antarctic Science*, *9*(2), 201–208, 1997.
- King, M., The Dynamics of the Amery Ice Shelf From a Combination of Terrestrial and Space Geodetic Data, Unpublished Ph.D. Thesis, University of Tasmania, 386 pp., 2001.
- Martin, T. V., A. C. Brenner, H. J. Zwally, and R. A. Bindschadler, Analysis and retracking of continental ice sheet radar altimeter waveforms, *J. Geophys. Res.*, *88*, 1608–1616, 1983.
- Padman, L., H. A. Fricker, R. Coleman, S. L. Howard, and L. Erofeeva, A new tide model for the Antarctic ice shelves and seas, *Ann. Glaciol.*, *34*, in press, 2002.
- Padman, L., and C. Kottmeier, High-frequency ice motion and divergence in the Weddell Sea, *J. Geophys. Res.*, *105*, 3379–3400, 2000.
- Ray, R. D., and B. V. Sanchez, Radial deformation of the earth by oceanic tidal loading, NASA Tech. memo. 100743, Goddard Space Flight Center, 1989.
- Rignot, E., and D. R. MacAyeal, Ice-shelf dynamics near the front of Filchner-Ronne Ice Shelf, Antarctica, revealed by SAR interferometry, *J. Glaciol.*, *44*(147), 405–418, 1998.
- Rignot, E., L. Padman, D. R. MacAyeal, and M. Schmeltz, Observation of ocean tides below the Filchner and Ronne Ice Shelves, Antarctica, using SAR: Comparison with tide model predictions, *J. Geophys. Res.*, *105*, 19,615–19,630, 2000.
- Robertson, R. A., L. Padman, and G. D. Egbert, Tides in the Weddell Sea, in *Ocean, Ice, and Atmosphere: Interactions at the Antarctic Continental Margin*, edited by S. S. Jacobs and R. F. Weiss, Antarctic Research Series, vol. 75, 341–369, 1998.
- Scott, R. F., et al., A comparison of the performance of ice and ocean tracking modes of the ERS-1 radar altimeter over non-ocean surfaces, *Geophys. Res. Lett.*, *21*(7), 553–556, 1994.
- Shum, C. K., et al., Accuracy assessment of recent ocean tide models, *J. Geophys. Res.*, *102*, 25,173–25,194, 1997.
- Smith, A. J. E., Application of satellite altimetry for global ocean tide modeling, Ph.D. Thesis, Delft University press, Delft, The Netherlands, 182 pp., 1999.
- H. A. Fricker, Institute of Geophysics and Planetary Physics, Scripps Institution of Oceanography, University of California, San Diego, La Jolla, CA 92093-0225, USA.
- L. Padman, Earth and Space Research, 1910 Fairview Ave. E., Suite 102, Seattle, WA 98102-3620, USA.